Chemical-state-resolved x-ray standing-wave analysis of Te-adsorbed GaAs(001)-(2×1) surface

Munehiro Sugiyama and Satoshi Maeyama
NTT Basic Research Laboratories, 3-1 Morinosato, Wakamiya, Atsugi, Kanagawa 243-01, Japan
(Received 19 June 1997; revised manuscript received 15 September 1997)

A Te-adsorbed GaAs(001)-(2×1) surface is studied by back-reflection x-ray standing-wave analysis, and average position of adsorbed Te atoms on GaAs(001) is found to be close to the As atomic site and bond with Ga atoms. Chemical-state-resolved x-ray standing-wave analysis using chemical shift in Te $3d_{5/2}$ core-level photoelectron spectra suggest that Te atoms in two different chemical states correspond to two different distributions. Te atoms in a lower binding-energy chemical state are found to be in higher atomic positions and to be less ordered, whereas those in a higher binding-energy chemical state are found to be in lower atomic position and are highly ordered. [S0163-1829(98)00811-X]

The behavior of group-VI elements (S, Se, Te) on GaAs surfaces is technologically important because this may play an important role in the chalcogen passivation treatments of GaAs surfaces,[1,2] the heteroepitaxial growth of II–VI semiconductors and I-III-VI_2 chalcopyrite semiconductors[3] on GaAs surfaces, and the fabrication of quantum dot structure on chalcogen-treated GaAs surfaces.[4] One of the Te-contained compounds epitaxially grown on GaAs surfaces is $Hg_{1-x}Cd_xTe$, which is a prime candidate for photodetectors in the 8–12-μm spectral region. Thus, the molecular-beam-epitaxy (MBE) growth of $Hg_{1-x}Cd_xTe$ on GaAs substrate has been studied for a long time. On the other hand, Spahn *et al.*[5] examined the Te-termination effects on ZnSe growth on GaAs(001) surface, and found that half a monolayer of Te-terminated substrate showed a two-dimensional ZnSe growth start, pseudomorphic growth up to 400 nm, good crystalline quality, and reproducible electrical behavior. The layer-by-layer ZnSe growth on Te-terminated GaAs(001) surface was also confirmed by Ohtake *et al.*[6]

Compared to S- and Se-adsorbed GaAs(001) surfaces, the structures of Te-adsorbed GaAs(001) surface are not fully understood. Gobil and co-workers[7] obtained phase diagrams of the different surface superstructures, and reported that (2×1) reconstructed Te-adsorbed GaAs(001) surfaces can be produced by heating GaAs(001)-(2×4) clean surface at 400 °C under Te flux. They also reported that there are two distinct chemical states in the Te 3*d* x-ray photoelectron spectrum for the Te-adsorbed GaAs(001)-(2×1) surface. Etgens *et al.*[8] studied the structure of this Te-adsorbed GaAs(001)-(2×1) surface by grazing incidence x-ray diffraction and constructed a structure model based on the previous reports given by Gobil and co-workers.[7] X-ray photoelectron diffraction study of Te-adsorbed GaAs(001)-(1×1) surface, which was made by exposing the surface to 50 ppm of $(C_2H_5)_2Te$ at 60 Torr diluted in H_2 for 10 min, was reported by Chambers and Sundaram.[9] They also observed two distinct chemical states in Te 3*d* photoelectron spectra. Biegelsen *et al.*[10] observed a scanning tunneling microscope (STM) image of a Te-adsorbed GaAs(001) surface, and found that long rows running in the [110] direction with 0.8-nm spacing show a strong tendency to repel each other. Ohno[11] calculated total energies for four possible adsorption sites, such as the bridge, on-top, antibridge, and hollow sites, on the Ga-terminated GaAs(001) surface and concluded that Te atoms are at the bridge site.

The x-ray standing-wave (XSW) technique is capable of locating the position of particular atomic species at a crystal surface.[12] After the advantages of a back-reflection x-ray standing-wave technique by scanning the photon energy were pointed out by Woodruff *et al.*,[13] several studies utilizing this technique have been reported. When structures of the adsorbates on III-V compound semiconductor surfaces have been analyzed by XSW, the group-III atomic site and the group-V atomic site can be distinguished by using noncentrosymmetric {111} reflections. Therefore, two different XSW experiments of (111) and (111) reflections are thought to be suitable for the analysis of GaAs(001) surface.[14–16] On the other hand, we have demonstrated the chemical-state-resolved XSW techniques. One is the near-edge XSW, which is an extension of the XSW technique by utilizing the chemical sensitivity of the fluorescent x-ray yield near the absorption edge of a target element.[17] However, a slight difference in chemical states cannot be resolved by this technique. The other is the photoemission spectroscopy XSW technique that combines x-ray photoelectron spectroscopy and XSW.[18]

A (2×1) reconstructed Te-adsorbed GaAs(001) surface was prepared as follows. After the chemical treatment, an *n*-type GaAs(001) wafer was attached to an Mo sample holder with an In solder and transferred to a MBE growth chamber. The sample surface was flashed to 620 °C and then annealed for 15 min at 590 °C under an As flux to remove surface oxides and contamination. Next, the substrate temperature was immediately decreased to 560 °C and then GaAs was grown homoepitaxially. After the growth, the sample showed a sharp, streaky (2×4) reflection high-energy electron diffraction (RHEED) pattern. Several monolayers of Te atoms were deposited on the As-stabilized GaAs(001) surface at room temperature. The substrate temperature was increased to 450 °C and a (2×1) reconstructed surface was obtained as shown in Fig. 1 with the result of Te desorption and an exchange reaction between As and Te atoms at the surface. The (2×1) reconstructed Te/GaAs(001) surface is thought to be the same as that reported by Gobil *et al.*[7] This phenomena is thought to be very similar to that for an *in situ* S-treated GaAs(001) surface.[19] The sample was

 © 1998 The American Physical Society

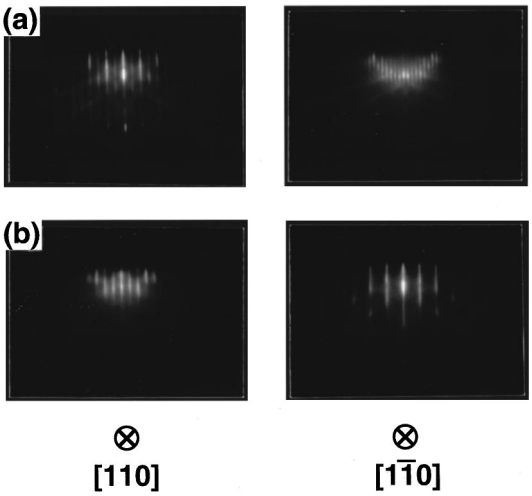

FIG. 1. RHEED patterns (a) before and (b) after Te adsorption on GaAs(001) surface. A (2×1) reconstructed Te/GaAs(001) surface was obtained by depositing Te atoms on GaAs(001)-(2×4) surface at room temperature followed by annealing at 450 °C.

transferred from the MBE chamber to the XSW analysis chamber through an ultrahigh vacuum.

The back-reflection XSW experiments were carried out at the NTT beamline 1A of the Photon Factory at the National Laboratory for High-Energy Physics.[20] We developed an ultrahigh vacuum three-axis goniometer system to perform XSW experiments.[21] In order to determine the three-dimensional arrangement of the Te atoms, back-reflection XSW experiments of both GaAs (111) and (111) reflections were performed by scanning a pair of InSb(111) crystals through the GaAs (111) and (111) normal-incidence Bragg reflection conditions, which occur at around 1.9 keV. For the GaAs(001) substrate, both the (111) and (111) diffraction planes were inclined at about 54° to the (001) surface. Thus, the (111) experiment could be set up by rotating the ϕ axis of the goniometer 90° after the (111) reflection experiment. These two XSW experiments were performed using the same arrangement. Te $3d_{5/2}$ core-level photoelectron spectra were collected at all data points using a 100-mm mean radius hemispherical electron energy analyzer (CLAM2) with a lens unit. Background subtraction and peak separation were carried out after the measurement.

Figure 2 shows Te $3d_{5/2}$ spectra under five different conditions around the (111) reflection. Gobil *et al.*[7] showed an XPS spectrum of the Te $3d_{5/2}$ peak for a Te-adsorbed GaAs(001)-(2×1) surface and their deconvolutions using Gaussian line shapes. They found two distinct chemical components in the Te $3d_{5/2}$ spectrum separated by 0.9 eV for the Te-adsorbed GaAs(001)-(2×1) surface. In the Te $3d_{5/2}$ peak separation shown in Fig. 2, Te $3d_{5/2}$ spectra were deconvoluted by using two peak positions (573.0 and 572.1 eV in binding energy) as pointed out by Gobil *et al.*[7] They pointed out that accuracy of these peak positions are estimated to be about 0.2 eV. Therefore, we have tried different peak positions to estimate how these peak positions affect the results of the XSW analysis, and showed roughly estimated errors of our chemical-state-resolved XSW analysis in the latter part of discussion in this paper. Two line shapes (90% Gaussian plus 10% Lorentzian) with 1.4 eV full width

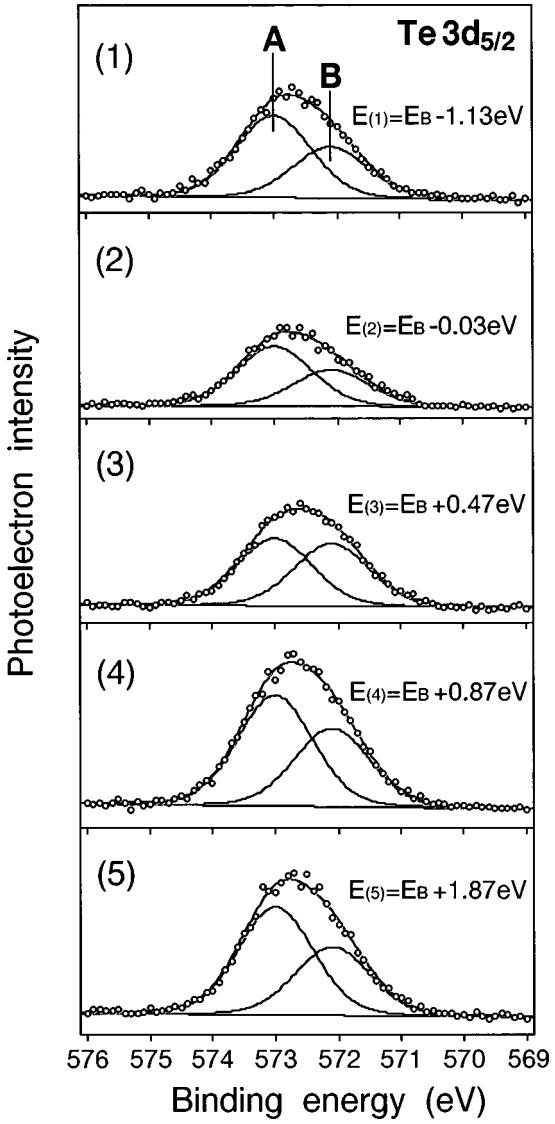

FIG. 2. Te $3d_{5/2}$ photoelectron spectra collected under the five different photon energies around the (111) Bragg condition. The relative photon energies E to the energy of the (111) back-reflection Bragg condition E_B (1.9 keV) are shown in this figure. Integrated intensities of these spectra (1)–(5) are shown in Fig. 3 as the (111) XSW data points (1)–(5). Vertical axis is the photoelectron intensity normalized by the incident x-ray intensity. The intensity of the Te $3d_{5/2}$ photoelectron peak at the off-Bragg condition was about 700 counts, and the error bars of the data points are the same order of the size of the circles.

at half maximum (FWHM) were used to fit the observed spectra in this study. This width is slightly wider than that observed by Gobil *et al.* using Al $K\alpha$ source. This is because the energy resolution of incident photons of about 1.9 keV in this study is wider than monochromatized Al $K\alpha$ source used by Gobil *et al.*[7] In the peak deconvolution, the ratio of the two chemical components A and B was found to be about 60% and 40%, respectively, in the off-Bragg conditions. If there is no difference in the distribution of Te atoms in these two chemical states, the shape of the Te $3d_{5/2}$ spectra should not change except for the peak intensity and its background level. However, it was found that there are significant changes in the shape of the peaks. This indicates that the

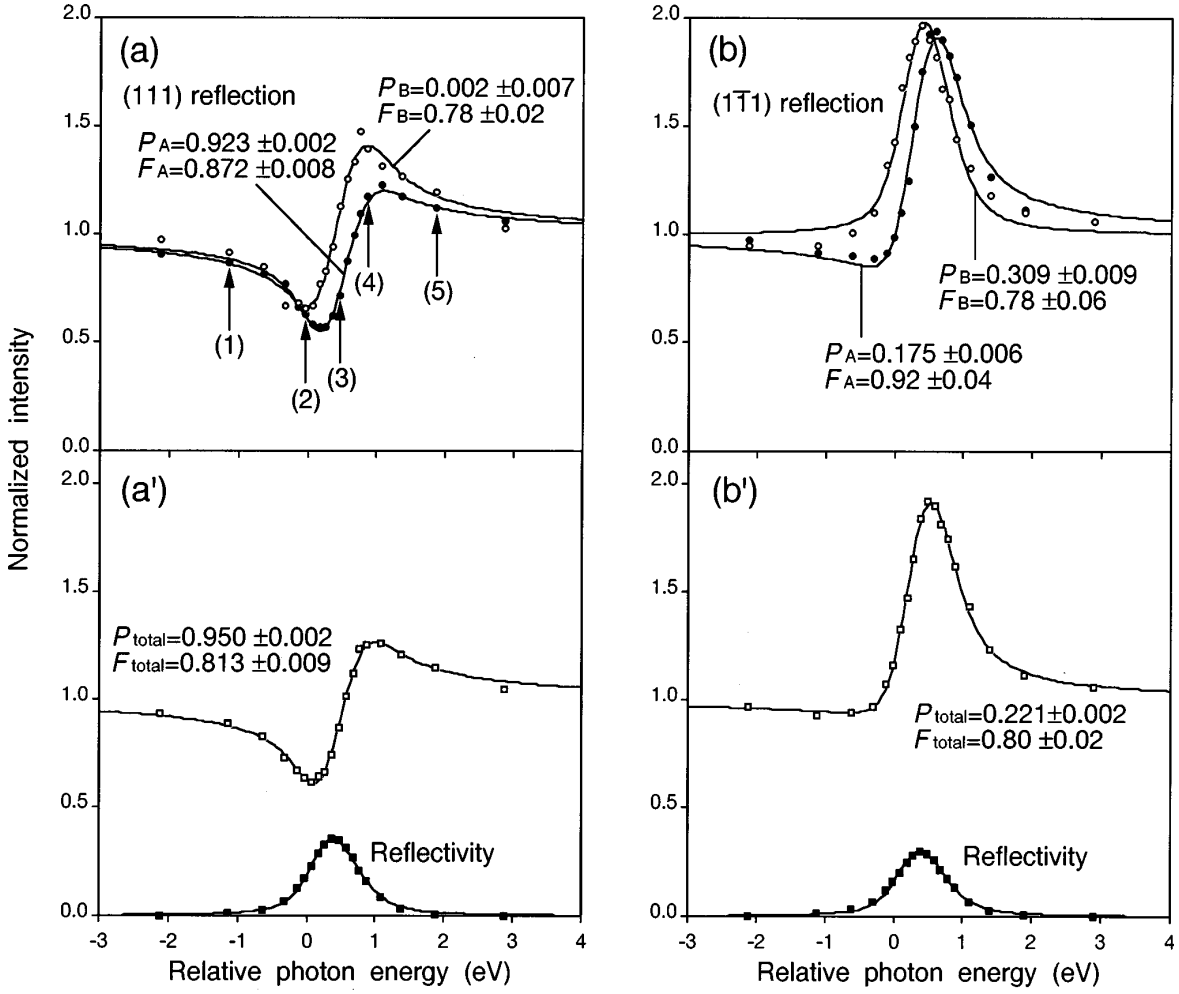

FIG. 3. Chemical-state-resolved back-reflection XSW results of two reflections: (111) and ($1\bar{1}1$) reflection. The horizontal axis is the relative energy of incident photons to the Bragg reflection energy at the normal incidence. The solid squares are the Bragg reflection. The open squares are the total Te $3d_{5/2}$ photoelectron intensity data. The solid and open squares are chemical components A and B, respectively. Te $3d_{5/2}$ data points (1)–(5) in the (111) result correspond to Te $3d_{5/2}$ spectra (1)–(5) in Fig. 2. Although real values of error bars for open squares are thought to be larger than the size of the squares, statistical error values estimated by the R factors were smaller than the size of the squares.

distribution of Te atoms in chemical state A and B must be different. In order to investigate the distribution in each chemical state, integrated intensities of chemical state A and B are independently analyzed in this chemical-state-resolved XSW study.

In the back-reflection XSW analysis, the photon-energy-dependent secondary-emission yield profile, $Y_{(E)}$, is given by

$$Y_{(E)}=1+R_{(E)}+2F\sqrt{R_{(E)}}\cos(2\pi P-\delta_{(E)}), \qquad (1)$$

where $R_{(E)}$ is the intrinsic reflectivity and $\delta_{(E)}$ the phase between the two plane waves that form the interference field. Here, $R_{(E)}$ in the back-reflection condition and $\delta_{(E)}$ can be computed as a function of photon energy E. We used the anomalous atomic scattering factors reported by Henke *et al.*[22] and the room-temperature Debye-Waller factors of the Ga and As atoms calculated from B values reported by Stevenson.[23] The two parameters P and F in Eq. (1), which can be determined by the XSW analysis, are called the coherent position and the coherent fraction, respectively. These parameters contain structural information about target atoms. The coherent position P gives the position of the target atoms with respect to the specific bulk-extrapolated reflection planes. In our case, the coherent position P is defined as the normal distance in units of the GaAs{111} d-spacing from the {111} net planes, which lie at the midpoint of the Ga-As double layers. The coherent fraction F includes both the Debye-Waller factor and the fraction of the atoms at the actual lattice sites defined by the coherent position P. In other words, the coherent fraction F acts as a measure of the degree of ordering. A highly disordered, or amorphous distribution, corresponds to F of 0. On the other hand, F close to 1 indicates that all target atoms are almost at identical positions.

Figure 3 shows normal and chemical-state-resolved XSW results for the (2×1) reconstructed Te-adsorbed GaAs(001) surface. (1)–(5) in Fig. 2 correspond to (1)–(5) in Fig. 3(a). Theoretical curves were convoluted by instrumental resolution function of 80% Gaussian and 20% Lorentzian, whose FWHM is 0.5 eV. The coherent position P and the coherent fraction F were determined for total and partial Te $3d_{5/2}$ photoelectron intensity profiles from least-square fits to the

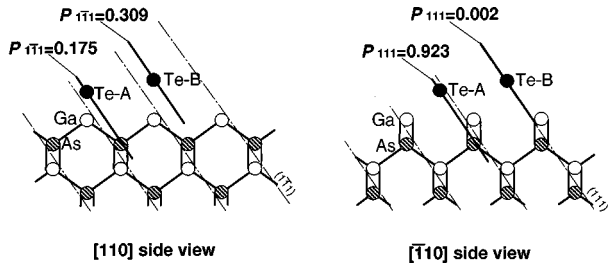

FIG. 4. Schematic side views showing adsorption positions of Te atoms (solid circles) with respect to GaAs lattice unit cell. The XSW results give normal distances from the specific bulk or bulk-extrapolated reflection net planes. We defined that the (111) and (111) net plane lie at the middle position of the As-Ga and Ga-As double layers, respectively. Two different Te atomic positions correspond to two different chemical states of Te atoms.

theoretical profiles. The determined P and F values are indicated in Fig. 3. The P values determined for total Te $3d_{5/2}$ photoelectron intensity profiles give a position close to the As site. The P values determined for chemical state A give the position that is lower than that for the total, and the P values determined for chemical state B give a position that is higher than that for the total. These results suggest that adsorption sites of Te atoms are close to the As site as predicted by the theoretical study.[11] Gobil and co-workers[7] assigned two Te $3d_{5/2}$ peaks as Te-As and Te-Te chemical states. However, our chemical-state-resolved XSW results revealed that most Te atoms stay at the As site and form Te-Ga bonds on the Te-adsorbed GaAs(001)-(2×1) surface. We concluded that Te-Ga bonds are dominant on this surface, and the two distinct chemical components in Te $3d_{5/2}$ photoelectron spectra correspond to two different vertical heights with respect to the ideal GaAs lattice unit cell. This is supported by the experimental results for a similar system of Se-treated GaAs(001)-(2×1) surface, in which there are also two distinct chemical states in the Se $3d$ core-level spectra.[24] Both of these chemical states are thought to be Se-Ga chemical states.[25] It should be noted that our results are not consistent with a structure model revealed by x-ray diffraction.[8] This was based on the assumption previously reported by Gobil and co-workers.[7]

TABLE I. Atomic positions of Te adsorbates on GaAs(001) surface determined by chemical-state-resolved XSW results.

		P_A	$D_{\mathrm{Te}_{(A)}\text{-Ga}}$
A	$(1\bar{1}1)$	0.923 ± 0.002	1.68 ± 0.01 Å
	(111)	0.175 ± 0.006	1.70 ± 0.03 Å
		P_B	$D_{\mathrm{Te}_{(B)}\text{-Ga}}$
B	$(1\bar{1}1)$	0.002 ± 0.007	2.13 ± 0.04 Å
	(111)	0.309 ± 0.009	2.45 ± 0.05 Å

Figure 4 shows the Te adsorption sites revealed by the XSW analysis. The surface normal distance $D_{\text{Te-Ga}}$ between the position of Te atoms and the bulk lattice position of the underlying Ga atoms can be obtained from either P_{111} or $P_{1\bar{1}1}$. Table I shows P values determined by XSW analysis and $D_{\text{Te-Ga}}$ calculated from these P values. It should be noted that the larger difference in the atomic heights of Te atoms in chemical state B between (111) and $(1\bar{1}1)$ results may be caused by experimental and analytical errors. Actually, the chemical-state-resolved XSW data in Fig. 3(b) do not agree well with the calculated curves. It is thought that the (111) XSW results are more reliable than the $(1\bar{1}1)$ results in this study.

Here, different peak positions were assumed in the peak separation of Te core levels to estimate how these peak positions affect the results of the XSW analysis, and we roughly estimated errors of this chemical-state-resolved XSW analysis. Though it is thought that peak width and symmetry also affect the error values, peak position dependence was studied here. Table II shows five different peak deconvolution conditions. The closer the peak separation, the closer the determined P values were. Large analytical errors were observed in the chemical-state-resolved XSW analysis. This suggests that the analytical errors should be mainly caused by the peak separation of the broad Te $3d$ core-level spectra, and that error values for chemical states A and B written in Table I would not show the real analytical errors. Therefore, it should be noted that there may be errors more than a percent order of the unit cell in the P values determined by this chemical-state-resolved XSW analysis.

TABLE II. Te $3d$ peak separation condition dependence in the chemical-state-resolved XSW analysis.

			Assumed peak positions (in binding energy)				
			1	2	3	4	5
	A		573.0 eV	573.0 eV	573.0 eV	572.9 eV	573.1 eV
	B		572.1 eV	572.2 eV	572.0 eV	572.2 eV	572.0 eV
	R factor[a]		4.8%	5.2%	5.6%	7.4%	8.6%
(111)	A	P	0.923(2)	0.918(2)	0.927(2)	0.917(2)	0.926(2)
		F	0.872(8)	0.885(9)	0.862(7)	0.886(9)	0.863(7)
	B	P	0.002(7)	0.002(7)	0.002(6)	0.002(9)	0.991(5)
		F	0.78(2)	0.78(2)	0.77(2)	0.79(3)	0.78(2)
$(1\bar{1}1)$	A	P	0.175(6)	0.167(7)	0.182(5)	0.168(7)	0.180(5)
		F	0.92(4)	0.95(4)	0.90(3)	0.96(5)	0.90(3)
	B	P	0.309(9)	0.309(8)	0.308(9)	0.34(1)	0.291(7)
		F	0.78(6)	0.78(6)	0.77(6)	0.82(9)	0.76(5)

[a]These are the R factors for the same Te $3d$ spectrum shown in Fig. 2 (1).

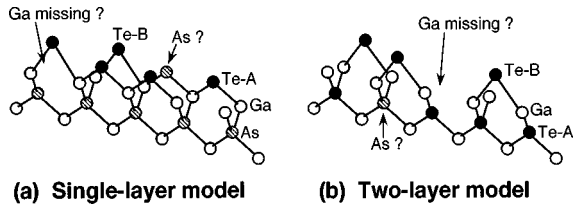

FIG. 5. Two possible structure models of Te GaAs(001)-(2 $\times$1) surface proposed in this study. With the XSW analysis results, we cannot distinguish an (a) single-layer model and a (b) two-layer model. The ratio of the two chemical components *A* and *B* was estimated to be about 60% and 40%, respectively. Detailed information about the ''Ga missing?'' and ''As?'' could not be given in this study, because the XSW analysis can only see the adsorbed species.

As noted in Table I, $D_{\text{Te-Ga}}$ for chemical state *A* was found to be 1.7 Å. This indicates that the Te atoms in chemical state *A* are about 1.7 Å above the underlying ideal Ga layer. Te-Ga bond length for chemical state *A*, calculated by using a simple Ga-Te-Ga bridge configuration and assuming no substrate lattice relaxation, was 2.61–2.62 Å. This is close to those in Ga_2Te_3 bulk crystal (2.55 Å) and in the bridge bond configuration determined by a theoretical study (2.56 Å). On the other hand, $D_{\text{Te-Ga}}$ for chemical state *B* was found to be more than 2 Å. Cohen-Solal, Bailly, and Barbe[26] proposed a twin tetrahedral structure. We propose two kinds of structure models as shown in Fig. 5. In model (a), two kinds of Te atoms which are in different chemical states exist on the surface, and the relatively larger $D_{\text{Te-Ga}}$ value for the chemical state can be explained. On the other hand, the relatively larger $D_{\text{Te-Ga}}$ value for the chemical state *B* may also be explained by an another model as shown in Fig. 5(b), in which a thin Ga_2Te_3 or GaTe layer with two Te atomic layers is formed on the surface. The $D_{\text{Te-Ga}}$ value for the upper layer must be larger than that for the lower layer, because the lattice constant of the Ga_2Te_3 bulk crystal is larger than that of GaAs. Actually, Ohtake *et al.*[6] reported that vacancy contained Ga_2Te_3-like interface layer exists after ZnSe layer is grown on a Te-terminated GaAs(001)-(6$\times$1) surface, though the atomic composition of the (6$\times$1) surface is different from that of the Te-terminated GaAs(001)-(2$\times$1) surface which we studied. It should be noted that we cannot conclude whether there are Ga vacancies near the surface or not. In both models, Te atoms bond with Ga atoms and occupy the As atomic site. Judging from the *F* values, Te atoms in the chemical state *A* are highly ordered, whereas those in chemical state *B* are less ordered. This difference in ordering degree may be related to the atomic arrangement of this surface. This significantly smaller *F* values for chemical state *B* may suggest that the two-layer model may be favorable, because the first layer is thought to be less stable than substitutional layer in the two-layer model shown in Fig. 5.

This surface has a (2$\times$1) reconstruction according to the RHEED pattern. The origin of this 2$\times$ periodicity may be Te-Te dimers or As-Te dimers or Te missing rows. The *F* value of the (111) XSW result for chemical state *A* was found to be very high, and the *F* values of both (111) and (111) XSW results for chemical state *B* were small, but almost the same. These results suggest that Te atoms in chemical state *A* distribute isotropically. Spahn *et al.*[5] reported that Te coverage on a Te-adsorbed GaAs(001) surface produced by exposure to Te flux (2.2×10^{-6} mbar) for 2 min at 300 °C is about half a monolayer. On the other hand, an STM image of the Te-adsorbed GaAs(001) surface reported by Biegelsen *et al.*[10] showed that long rows running in the [110] direction with 0.8-nm spacing show a strong tendency to repel each other. However, the chemical identities of the constituents of the rows could not be determined. Te-Te dimer and As-Te dimer structures with small aisotropical distribution of Te atoms, or Te missing row structure may be partly formed on this surface, but detailed information concerning the 2$\times$ periodicity has not yet been obtained. To obtain more detailed information about the structure of this surface, crystal truncation rod profile analysis of the x-ray diffraction pattern may be suitable.

In conclusion, the structure of a (2$\times$1) reconstructed Te/GaAs(001) surface, prepared by depositing Te atoms on GaAs(001)-(2$\times$4) clean surface and annealing at 450 °C was studied by chemical-state-resolved back-reflection XSW analysis using chemical shift in Te $3d_{5/2}$ core-level photoelectron spectra. Te atoms in two different chemical states were found to correspond to two different distributions on the GaAs(001) surface, even though those in both chemical states were close to the As sites and bonded with Ga atoms. The atomic height of Te atoms in the lower binding-energy chemical state (*B*) was found to be higher than that in the higher binding-energy chemical state (*A*). The ordering degree of the higher binding-energy chemical state (*A*) was higher than that of the lower binding-energy chemical state (*B*).

We thank Dr. W. Spahn of the Physikalisches Institut der Universitat Wurzburg, and Dr. A. Ohtake of the Joint Research Center for Atom Technology (JRCAT) for the valuable discussion about the Te-termination process and structure of Te-terminated GaAs(001) surfaces. We also thank Dr. Y. Watanabe of NTT Basic Research Laboratories for his helpful advice on the homoepitaxial growth of GaAs.

[1] C. J. Sandroff, R. N. Nottenbur, J. C. Bischoff, and R. Bhat, Appl. Phys. Lett. **51**, 33 (1987).

[2] Y. Nannichi, J. Fan, H. Oigawa, and A. Koma, Jpn. J. Appl. Phys., Part 2 **27**, L2367 (1988).

[3] For example, S. Niki, Y. Makita, A. Yamada, O. Hellman, P. J. Fons, A. Obara, Y. Okada, R. Shioda, H. Oyanagi, T. Kurafuji, S. Chichibu, and H. Nakanishi, J. Cryst. Growth **150**, 1201 (1995).

[4] N. Koguchi and K. Ishige, Jpn. J. Appl. Phys. **32**, 2052 (1993); T. Chikyow, S. Takahashi, and N. Koguchi, Surf. Sci. **267**, 241 (1992).

[5] W. Spahn, H. R. Ress, K. Schull, M. Ehinger, D. Hommel, and G.

Landwehr, J. Cryst. Growth **159**, 761 (1996); W. Spahn, H. R. Ress, C. Fischer, M. Ehinger, and G. Landwehr, Semicond. Sci. Technol. **12**, 234 (1997).

[6] A. Ohtake, L. H. Kuo, T. Yasuda, K. Kimura, S. Miwa, T. Yao, K. Nakajima, and K. Kimura, J. Vac. Sci. Technol. B **15**, 1254 (1997).

[7] Y. Gobil, J. Cibert, K. Saminadayar, and S. Tatarenko, Surf. Sci. **211/212**, 969 (1989); S. Tatarenko, J. Cibert, Y. Gobil, G. Feuillet, K. Saminadayar, A. C. Chami, and E. Ligeon, Appl. Surf. Sci. **41/42**, 470 (1989).

[8] V. H. Etgens, R. Pinchaux, M. Sauvage-Simkin, J. Massies, N. Jedrecy, N. Greiser, and S. Tatarenko, Surf. Sci. **251/252**, 478 (1991).

[9] S. A. Chambers and V. S. Sundaram, J. Vac. Sci. Technol. B **9**, 2256 (1991).

[10] D. K. Biegelsen, R. D. Bringans, J. E. Northrup, and L.-E. Swartz, Phys. Rev. B **49**, 5424 (1994).

[11] T. Ohno, Surf. Sci. **255**, 229 (1991).

[12] J. Zegenhagen, Surf. Sci. Rep. **18**, 199 (1993).

[13] D. P. Woodruff, D. L. Seymour, C. F. McConville, C. E. Riley, M. D. Crapper, and N. P. Prince, Phys. Rev. Lett. **58**, 1460 (1987).

[14] J. R. Patel, D. W. Berreman, F. Sette, P. H. Citrin, J. E. Rowe, P. L. Cowan, J. Jach, and B. Karlin, Phys. Rev. B **40**, 1330 (1989).

[15] J. C. Woicik, T. Kendelewicz, K. E. Miyano, P. L. Cowan, C. E. Bouldin, B. A. Karlin, P. Pianetta, and W. E. Spicer, Phys. Rev. Lett. **68**, 341 (1992).

[16] M. Sugiyama, S. Maeyama, F. Maeda, and M. Oshima, Phys. Rev. B **52**, 2678 (1995).

[17] M. Sugiyama, S. Maeyama, and M. Oshima, Phys. Rev. Lett. **71**, 2611 (1993).

[18] M. Sugiyama, S. Maeyama, and M. Oshima, Phys. Rev. B **51**, 14 778 (1995).

[19] S. Tsukamoto, and N. Koguchi, Jpn. J. Appl. Phys., Part 2 **33**, L1185 (1994).

[20] T. Kawamura, S. Maeyama, M. Oshima, Y. Ishii, and T. Miyahara, Rev. Sci. Instrum. **60**, 1928 (1989).

[21] M. Sugiyama, S. Maeyama, and M. Oshima, Rev. Sci. Instrum. **67**, 3182 (1996).

[22] B. L. Henke, E. M. Gullikson, and J. C. Davis, At. Data Nucl. Data Tables **54**, No. 2, (1993).

[23] A. W. Stevenson, Acta Crystallogr., Sect. A: Found. Crystallogr. **A50**, 621 (1994).

[24] S. Takatani, T. Kikawa, and M. Nakazawa, Phys. Rev. B **45**, 8498 (1992).

[25] F. Maeda, Y. Watanabe, T. Scimeca, and M. Oshima, Phys. Rev. B **48**, 4956 (1993).

[26] G. Cohen-Solal, F. Bailly, and M. Barbe, Appl. Phys. Lett. **49**, 1519 (1986).